Hindawi
Contrast Media & Molecular Imaging
Volume 2023, Article ID 9870974, 1 page
https://doi.org/10.1155/2023/9870974

Retraction

Retracted: Characterization of Clinical Symptoms of Cervical Spondylotic Myelopathy Based on DKI Imaging Parameter Ratios

Contrast Media & Molecular Imaging

Received 18 July 2023; Accepted 18 July 2023; Published 19 July 2023

This article has been retracted by Hindawi following an investigation undertaken by the publisher [1]. This investigation has uncovered evidence of one or more of the following indicators of systematic manipulation of the publication process:

(1) Discrepancies in scope
(2) Discrepancies in the description of the research reported
(3) Discrepancies between the availability of data and the research described
(4) Inappropriate citations
(5) Incoherent, meaningless and/or irrelevant content included in the article
(6) Peer-review manipulation

The presence of these indicators undermines our confidence in the integrity of the article's content and we cannot, therefore, vouch for its reliability. Please note that this notice is intended solely to alert readers that the content of this article is unreliable. We have not investigated whether authors were aware of or involved in the systematic manipulation of the publication process.

In addition, our investigation has also shown that one or more of the following human-subject reporting requirements has not been met in this article: ethical approval by an Institutional Review Board (IRB) committee or equivalent, patient/participant consent to participate, and/or agreement to publish patient/participant details (where relevant).

Wiley and Hindawi regrets that the usual quality checks did not identify these issues before publication and have since put additional measures in place to safeguard research integrity.

We wish to credit our own Research Integrity and Research Publishing teams and anonymous and named external researchers and research integrity experts for contributing to this investigation.

The corresponding author, as the representative of all authors, has been given the opportunity to register their agreement or disagreement to this retraction. We have kept a record of any response received.

References

[1] X. Tian, L. Zhang, H. Liu, X. Zhang, Y. Sun, and Y. Zhang, "Characterization of Clinical Symptoms of Cervical Spondylotic Myelopathy Based on DKI Imaging Parameter Ratios," *Contrast Media & Molecular Imaging*, vol. 2022, Article ID 7491565, 17 pages, 2022.

Hindawi
Contrast Media & Molecular Imaging
Volume 2022, Article ID 7491565, 17 pages
https://doi.org/10.1155/2022/7491565

Research Article

Characterization of Clinical Symptoms of Cervical Spondylotic Myelopathy Based on DKI Imaging Parameter Ratios

Xiaonan Tian, Li Zhang, Hongran Liu, Xuesong Zhang, Yingcai Sun, and Yujin Zhang

CT Department, The Third Hospital of Hebei Medical University, Shijiazhuang 050051, Hebei, China

Correspondence should be addressed to Li Zhang; 1764200062@e.gzhu.edu.cn

Received 25 July 2022; Revised 20 September 2022; Accepted 27 September 2022; Published 11 October 2022

Academic Editor: Sandip K. Mishra

In recent years, people's living conditions have significantly improved, and their lifestyles have been diversified. However, the incidence of various diseases has also increased with it, including cervical spondylotic myelopathy (CSM). Spinal cord cervical spondylosis is one of the spinal cord compression disorders that can be severely disabling and accounts for 10% to 15% of all cervical spondylosis. In this paper, DKI image processing technology is used to study the symptoms of cervical spondylosis, which is helpful to help them explore the symptoms and causes. The onset of cervical spondylosis has a longer period of time, and the period of conservative treatment will inevitably require a longer period of time. The clinical symptoms of cervical spinal cord compression are mainly pain, and after the cervical spinal cord nerve is compressed, ischemia and hypoxia will occur, the nerve sensitivity will increase, and the patient will have reflex neck muscle pain symptoms. This causes degeneration of the patient's intervertebral disc tissue, degeneration of facet joints, ossification of the posterior longitudinal ligament, and formation of spurs on the posterior edge of the vertebral body. The condition will become more complicated, so it is very important to identify the characteristics of the clinical symptoms of cervical spondylotic myelopathy to help patients with cervical spondylosis recover. This paper identifies the clinical symptoms of cervical spondylosis based on the parameter ratio method of Diffusional Kurtosis Imaging (DKI). The current state of diffusion kurtosis imaging and the treatment of cervical spondylosis and the treatment operation are introduced, and the image enhancement technology in medical imaging is used to analyze the disc herniation of each segment in the overflexion, neutral and hyperextension positions. After comparing the FA, MK, and MD values in the spinal cord between the normal group and the patient group, the results showed that the FA, MD and MK values in the patient group were lower than those in the normal group, and the findings showed that the MD and MK values were positively correlated with the JOA score, reflecting that as the clinical symptoms of spinal cervical spondylosis worsened. The size and number of cervical intervertebral disc bulge on the hyperextension image is obvious and the number increases (especially the C4/5, C5/6, and C6/7 intervertebral discs with greater mobility), and the highest is 0.82 and 27%, respectively.

1. Introduction

1.1. Background. The basic cause of cervical spondylotic myelopathy is cervical spine degeneration. Among the various structures of the cervical spine, cervical disc degeneration is considered to be the earliest. With the degeneration of the intervertebral disc, the decrease in water content, the decrease in height and the protrusion of the peripheral edge, the thickening and ossification of the posterior longitudinal ligament covering the back of the intervertebral disc, the bone hyperplasia at the edge of the vertebral body, and the corresponding increase in the interlaminar ligamentum flavum and intervertebral joint stress, the thickening of the ligament joint capsule, and the reduction of elasticity, resulting in the reduction of the diameter of the spinal canal, especially the reduction of the anteroposterior diameter; that is, the reduction of the sagittal diameter constitutes the static factor of spinal cord compression. The dynamic factor mainly refers to the stress and deformation of the spinal cord increased by the extension and flexion of the cervical spine. With the improvement in people's physical fitness, the average life expectancy is gradually increasing, the aging of the population is getting worse, and the incidence of orthopedic degenerative diseases

has risen sharply, especially in the age group over 60. However, the current age of onset also shows a significant trend of younger age. As a common disease in spinal surgery, cervical spondylotic myelopathy accounts for about 10% of cervical spondylosis and its harm is the most serious among different types of cervical spondylosis. The natural history of CSM is a gradual and progressive deterioration process that can be accompanied by a long asymptomatic period. Trauma, fatigue, and cold can induce rapid symptoms and worsening of the condition.

1.2. Significance. Cervical spondylotic myelopathy is due to the degeneration of the cervical intervertebral disc and the structural changes of adjacent bones and soft tissues that cause compression of the spinal cord and cause various symptoms and signs. Cervical spondylotic myelopathy, as the most harmful to human health in the classification of cervical spondylosis, can cause numbness of limbs, decreased mobility of hands, and unstable walking in the early stages. The late stage can cause severe neurological dysfunction, urinary incontinence, and eventually quadriplegia. The disability rate is high, which will cause a great mental and economic burden on the society and individuals. According to investigations, most of the cervical spondylotic myelopathy is not obvious and gradually aggravates. Serious clinical symptoms do not appear until the middle and late stages. The developmental outcome usually leads to irreversible damage to spinal cord function, which seriously affects the quality of human life. Therefore, the early diagnosis of cervical spondylotic myelopathy is very important, mainly based on clinical symptoms, signs, and necessary imaging examinations. DKI is a new model that better characterizes the non-Gaussian diffusion of water molecules, and it can reveal more precisely important information about local tissue microstructure and pathophysiological alterations, especially in regions where the tissue structure is predominantly inhomogeneous.

1.3. Related Work. The association between cervical imaging variables and the seriousness of spinal cervical spondylosis (CSM) is controversial. Ninomiya's study was designed to investigate the relationship of spinal radiological variables to the seriousness of CSM and the relationship between the cervical spine and other spinal pelvic radiological parameters. The cervical spinal column complaint ratio (CCCR) was assessed on sagittal magnetic resonance imagery. Clinical evaluation was performed using the Japanese Orthopaedic Association (JOA) scoring system to analyze the correlation between clinical and imaging parameters. JOA refers to the Japanese Orthopaedic Association assessment treatment score, which is primarily used to evaluate functional disorders in the human body. The results showed that the JOA score had the highest association with SVA ($r = -0.46$, $p < 0.01$). He concluded that the severity of CSM worsened with poor spinal alignment, such as increased SVA. Although the imaging parameters of the lumbar pelvis had no significant effect on the cervical alignment and the severity of CSM, an inverse correlation between the imaging parameters of the cervical thoracolumbar and the pelvis was observed. Therefore, the experimental design is more rigorous, and the practicality of the study is not great [1]. The purpose of the Chang H's study was to assess the efficacy of selective laminectomy and laminoplasty for multisegmental spinal cervical spondylosis through a review of its radiologic and diagnostic outcomes. He retrospectively analyzed 67 patients who received posterior laminectomy (LN) or laminoplasty (LP). Among them, 32 cases were LN and 35 cases were LP. Preoperative MRI was applied to assess preoperative compression of the spinal cord and postoperative enlargement of the spinal cord area and to analyze the differences in operative time, bleeding during surgery, and bleeding after surgery. The clinical outcomes were analyzed using the Neck Disability Index (NDI) and the Visual Analog Scale (VAS) for neck pain. The Visual Analog Scale is used for the assessment of pain. Surgery was performed at the 2.04 level in the LN group and at the 4.06 level in the LP group. In the last following, the findings showed a significant reduction in Cobb angle and ROM in the LN group, with no difference in the rate and extent of preoperative spinal cord compression. But the experimental results have not been widely used [2]. Massel et al.'s research aims to conduct a retrospective database review. The purpose is to determine whether a dural tear will increase the cost of recovery during the initial lumbar discectomy and the risk of wound complications for elderly medical insurance beneficiaries. Research data show that the incidence of occasional durotomy during lumbar spine surgery is 1% to 17%, but the depth of research is not enough [3]. Yu et al.'s study reports a patient with severe unilateral semidiaphragmatic acute palsies and respiratory difficulty caused by spinal cervical spondylosis (CSM). The overall picture was that of an 82-year-old male patient who presented with unhelpful coarse cough, tightness in the chest, hissing voice, and tachypnea while walking. The man received a heart tube insertion, which revealed widespread narrowing of the heart artery. He consequently had a triple crown collateral graft. In spite of the cardiac procedure, the patient's respiratory distress did not resolve. The patient received a C2–C6 splint excision and fusion with a local autogenous bone graft. After the operation, the patient's dyspnea gradually eased and his physical strength also improved, and the dyspnea was completely relieved. Dyspnea may be related to unilateral diaphragmatic paralysis caused by CSM, and there is a lack of research on the multiple populations of the disease in the overall research content [4]. A major drawback of CSM management is the dearth of validated methods of diagnosis to tier treatment and forecast outcomes. Currently, there is no clinical diagnostic imaging method that accurately reflects the underlying spinal cord pathology. Murphy et al. used diffusion-based spectroscopic imaging (DBSI) to assess axonal/myelin damage, cellular inflammation, and arbor losses in the myelinated cervical cord quantitatively. Given the small number of severely ill patients, patients with moderate to severe cases were compared with seven age-matched controls and statistically analyzed. A new DBSI was developed to quantify axonal and myelin damage, cellular inflation, and loss of axons. The median inflammatory

volume of the DBSI was similar in the control group, but the experimental data were too few and not very convincing [5]. Anterior cervical discectomy and fusion have a good therapeutic effect on cervical spondylotic myelopathy. Wang et al. reviewed the outcomes of 32 consecutive patients that received 4-segment cervical anterior discectomy fusion (ACDF) with a minimum of 5 years of follow-up. The records of 19 men and 13 women between the ages of 48 and 69 years were reviewed. They were performed at 4 levels of ACDF for myelopathy ($n = 11$) and spinal radiculopathy ($n = 21$) by a surgeon from C3 to C7, and they were followed up for at least 5 years. The visual analog scale (VAS), the neck disability index (NDI), and the modified Japanese Orthopaedic Association (JOA) myelopathy symptom score were used to evaluate the clinical results. Imaging evaluation includes fusion rate, range of motion, cervical lordships (C2–C7 Cobb angle), and disc height. However, relatively few studies based on DKI imaging parameters than the direction of research on spinal cervical spondylosis are not thorough enough, and there is a need to fully apply these techniques to this field of research.

1.4. Innovation. As part of a dynamic study, this group selected the most important factors contributing to the development of cervical spondylosis and the size of the herniated disc. A large amount of data on the size of individual disc segments was measured at dynamic locations, and the size of herniated discs was comprehensively analyzed. The dynamic factors of occurrence and development of cervical spondylosis combine static MRI examination with dynamics and provide a comprehensive analysis of dynamic MRI changes in the normal cervical spine for the size of herniated discs. It reflects the worsening of clinical symptoms of cervical spondylotic myelopathy.

2. Identification of Clinical Symptom Characteristics of Cervical Spondylosis Based on DKI's Parametric Scaling

2.1. Parameter Ratio Method of Diffusional Kurtosis Imaging (DKI). Cervical myelopathy is one of the pathological changes of spinal cord compression. The clinical manifestations vary with the degree, location, and extent of the affected spinal cord. Sensory disturbances are mostly irregular, and arm numbness is more common, but objectively, the superficial pain disturbance does not necessarily correspond to the dermatome dominated by the lesion, deep sensations are rarely affected, and there may be a sense of the chest or abdominal girdle, which is often accompanied by abdominal wall reflexes enhanced. The upper extremities are usually mainly damaged by the motor neuron pathways below. The hands are clumsy and weak, and it is manifested as difficulty in fine movements such as writing, tying shoelaces and buttons, and using chopsticks. Diffusion tensor imaging (DTI) is a technique that utilizes diffusion-weighted images in various orientations and is obtained by using the Bloch–Torrey formulation of the diffusion tensor image [6]. Since the diffusion of water in actual organisms is three-dimensional and the degree of diffusion varies in each direction, the same diffusion factor used to calculate the diffusion motion in different directions cannot provide an accurate description of the diffusion that may affect the judgement [7]. Therefore, in order to be able to better indicate the anisotropy of each water molecule in the organism, the description of voxel diffusion is extended to three-dimensional space and the second-order symmetry tensor is introduced to describe the diffusion of voxels in three-dimensional space. The diffusion direction of voxels can be expressed by the eigenvectors of the symmetry tensor. The diffusion anisotropy fraction of each voxel is obtained by using the eigenvalues of the tensor matrix, which is also called the isotropy index [8]. The anisotropy fraction has different values in different tissues of the human body and varies greatly between lesioned and normal areas in the same tissue. With the rapid advancement of diffusion tensor imaging, the processing techniques for diffusion tensor imaging include image processing methods such as denoising of gradient images, deartifacting of sequence images, and alignment and interpolation between sequence images and between gradient images [9]. Figure 1 shows the processing flow of diffusion tensor imaging data, including preprocessing, imaging calculation, alignment, interpolation, region of interest selection, and clinical index calculations.

With the increasing sophistication and maturity of various MRI (magnetic resonance imaging) techniques, their use in assessing the extent of spinal cervical spondylosis is increasing and their advantages are becoming more apparent. Conventional MRI has limitations in determining spinal cord injury in CSM. DTI is based on the assumption that water molecules diffuse in a free, unrestricted form, i.e., the diffusion displacement is Gaussian distributed. The introduction of DKI can more objectively quantify the deviation between the actual non-Gaussian diffusion displacement of water molecules and the ideal state Gaussian diffusion displacement of water molecules. DKI is a new MRI technique based on diffusion tensor imaging, which utilizes the arbitrary diffusion of water molecules in a non-Gaussian model without the need to measure the diffusion displacement and distribution probability and therefore requires less imaging time and gradient hardware. The characteristic parameter of DKI, kurtosis (K), is used to quantify the deviation of the diffusion displacement of real non-Gaussian distributed water molecules from the ideal Gaussian distributed water molecules in living tissues, thus detecting the degree of diffusion restriction of water molecules in living tissues. The degree of diffusion restriction and diffusion inhomogeneity of water molecules within the living body are used to provide a more realistic picture of the complex microstructure and biological properties of the tissue [10].

The parameters specific to DKI include mean kurtosis (MK), kurtosis anisotropy (KA), axial kurtosis (AK, Ka, K//), and radial kurtosis (RK, Kr, K⊥). In addition, parameters of DTI such as fractional anisotropy (FA), mean diffusion (MD), axial diffusion tensor (AD, Da, D//), and vertical diffusion tensor (RD, Dr, and D⊥) can also be obtained in

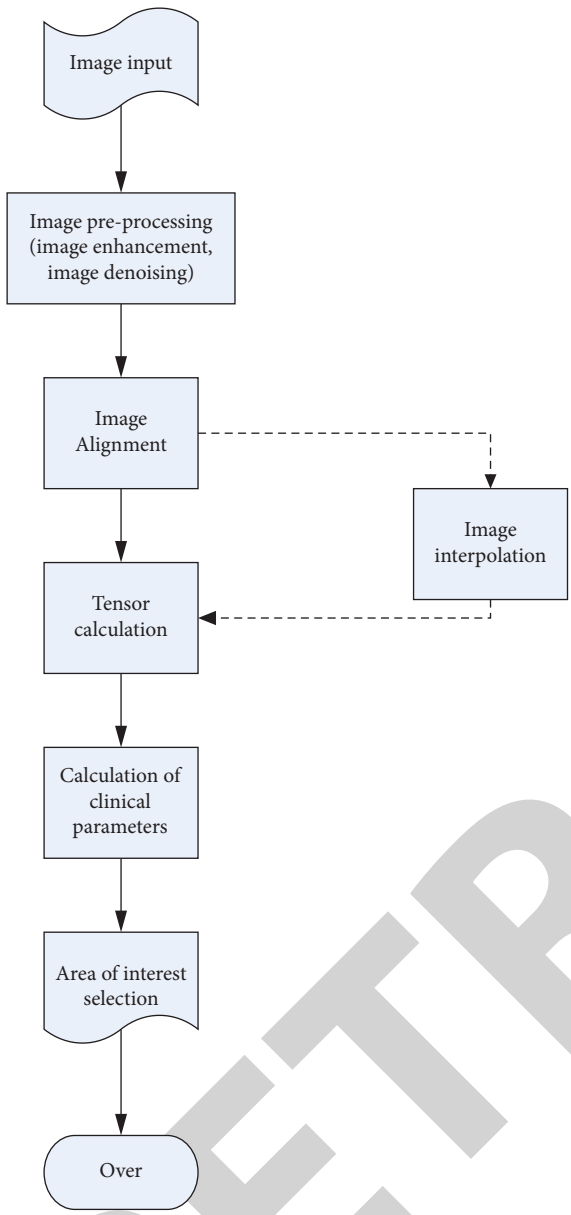

Figure 1: Diffusion tensor imaging data processing flow.

DKI. The advantage of MK is that it does not depend on the spatial orientation of the tissue structure, and both gray matter and white matter structures can be described by applying the mean kurtosis. The mean kurtosis (MK) is a measure of the complexity of the tissue structure in the region of interest and indicates the average value of the diffusion kurtosis of water molecules along all diffusion directions, reflecting the degree of restricted diffusion of water molecules. Therefore, the microstructural and pathological conditions of neural tissue altered in these two parameters are particularly prominent in the fine assessment of the spinal gray matter. At present, the decrease in MD value and the decrease in MK value in CSM can be used as valid diagnostic modalities, and these two indices will be selected as study parameters in this paper.

2.2. Digital Imaging Techniques and Image Preprocessing

2.2.1. Basic Concepts. The radiation dose required for digital imaging can be drastically reduced. The range density resolution of traditional X-ray imaging is low, the digital imaging density resolution is high, and the imaging latitude is large. Images obtained by conventional X-ray imaging cannot be postprocessed. Digital imaging can perform various postprocessing such as window width and window level adjustment, edge enhancement, and grayscale transformation. Images obtained by conventional X-ray imaging cannot be directly fed into the image storage and transmission systems, whereas digital imaging may be possible. The time for digital imaging to obtain image data is short, and the general digital imaging device can obtain 8 frames of images per second. In essence, an image is a collection of a large amount of information, and it is also the most important source for people to obtain information. But under normal circumstances, people cannot directly use the directly acquired images but need to adopt certain methods to process them, and computer technology is one of the most important methods. The computer system deals with digital images, which are actually a two-dimensional matrix composed of quantized samples of the image [11, 12]. The digital image is composed of multiple areas divided into different pixels. Each area has two different characteristics of grayscale and position. Digital imaging NDT methods have the advantage of high efficiency and low cost. After all the pixels in the image are quantified, the image is presented in the form of a digital matrix for the computer to process. The various processing techniques used for it are called digital imaging techniques. In short, digital imaging technology is the process of converting the analog signal of an image into a digital signal and using a computer to process the digital image. Since the gradual development of digital image technology, image processing technology has played an increasingly important role in medical imaging [13]. Figure 2 is the digital imaging unit flow.

2.2.2. Digital Image Processing Methods and Technologies. The digital processing of images refers to the conversion of images in analog format to images in digital format and then corresponding image processing according to a specific mathematical model structure to meet the requirements [14]. A new type of sensor that is developing rapidly in the world is called an imaging spectrometer, which is an instrument that acquires image information in a multichannel, continuous, and high spectral resolution manner. By organically combining the traditional spatial imaging technology with the ground object spectral technology, it is possible to obtain the ground object reflectance spectral images of dozens to hundreds of bands in the same area at the same time. Imaging spectrometers are basically multispectral scanners, and their structure is the same as that of CCD line array push-broom scanners and multispectral scanners. The only difference is that the number of channels is large, and the band width of each channel is very narrow.

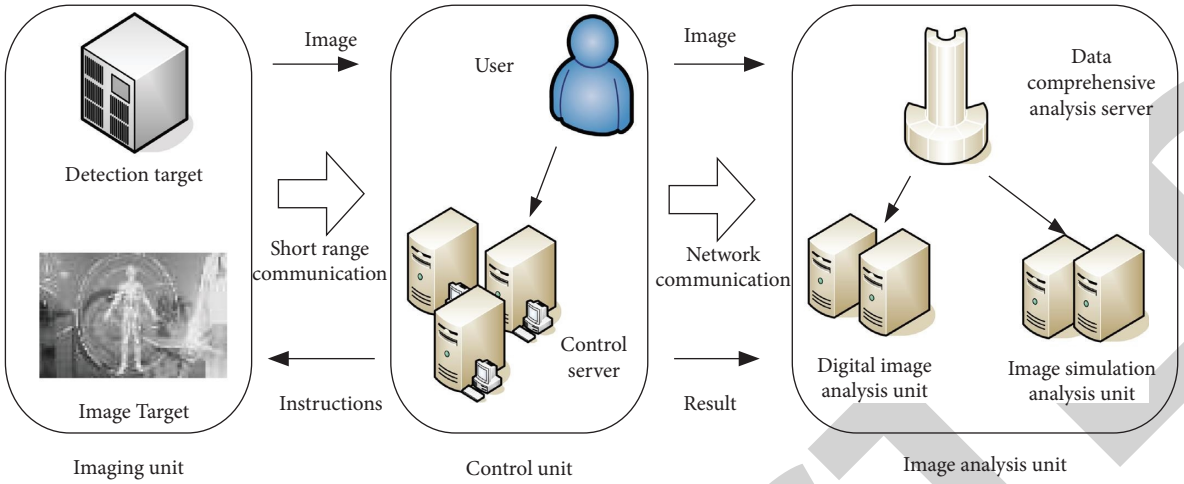

Figure 2: Flow chart of the digital imaging unit.

The research of digital image analysis and processing can be divided into the following three stages, as shown in Figure 3.

Among them, digital image processing mainly refers to various technical processing of images to enhance the effect of the image and provide a basis for subsequent image recognition and understanding. The main purpose of image processing is to eliminate inconsistencies, eliminate image noise, and improve image clarity [15]. The focus of image processing is image input and image preprocessing, as shown in Figure 4.

Image preprocessing is a key step in subsequent image segmentation and feature recognition. Its two main directions are nonuniformity correction and image enhancement [16]. Image enhancement refers to emphasizing image features (such as edges, pages, and contrast), so that important parts of the image are improved, and these features are easier to recognize [17]. The division of image enhancement methods is shown in Figure 5.

Noise pollution is generated when lines are acquired and transmitted, and image quality is inevitably degraded. Image enhancement technology is the most basic type of image processing technology. Its ultimate purpose is to emphasize the feature information in the image and to expand the features of different elements in the image by filtering out some unnecessary parts of the image [18]. The basic principle of image enhancement is to purposely emphasize the overall or local characteristics of an image, to make the original unclear image clear or to emphasize certain features of interest, to expand the differences between different object features in the image, and to suppress the features of no interest. Image enhancement techniques primarily consist of gray level contrast conversion, histogram calibration, smoothing of images, image sharpening, etc. There are two types of image intensification methods: space field enhancement and spectrum field enhancement [20]. Spatial-domain enhancement is to directly adjust the gray level of the image, use parameter ratio enhancement, and obtain a new ratio image through the ratio between the brightness of different groups of pixels. Methods such as increasing the contrast of the image and increasing the gray level are all

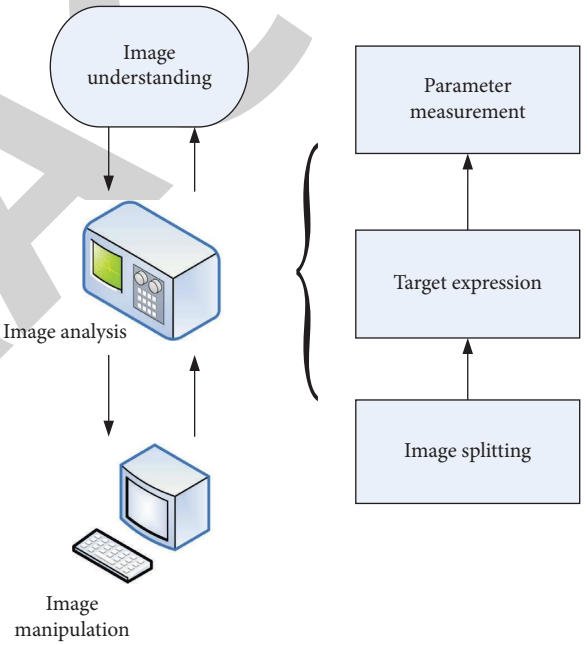

Figure 3: Research level of digital image processing.

spatial-domain enhancements. Frequency-domain enhancement is the processing of images in the frequency-domain range. The main principle is to use Fourier transform and inverse transform to transform the space domain and frequency domain.

Generally speaking, there are three main purposes of image processing: improve the visual quality of the image, such as image brightness, color transformation, enhancement, suppression of some components, and image geometric transformation, etc., to improve the image quality. Extract some features or special information contained in the image. These extracted features or information often provide convenience for the computer to analyze the image. The process of extracting features or information is a preprocessing of pattern recognition or computer vision. The

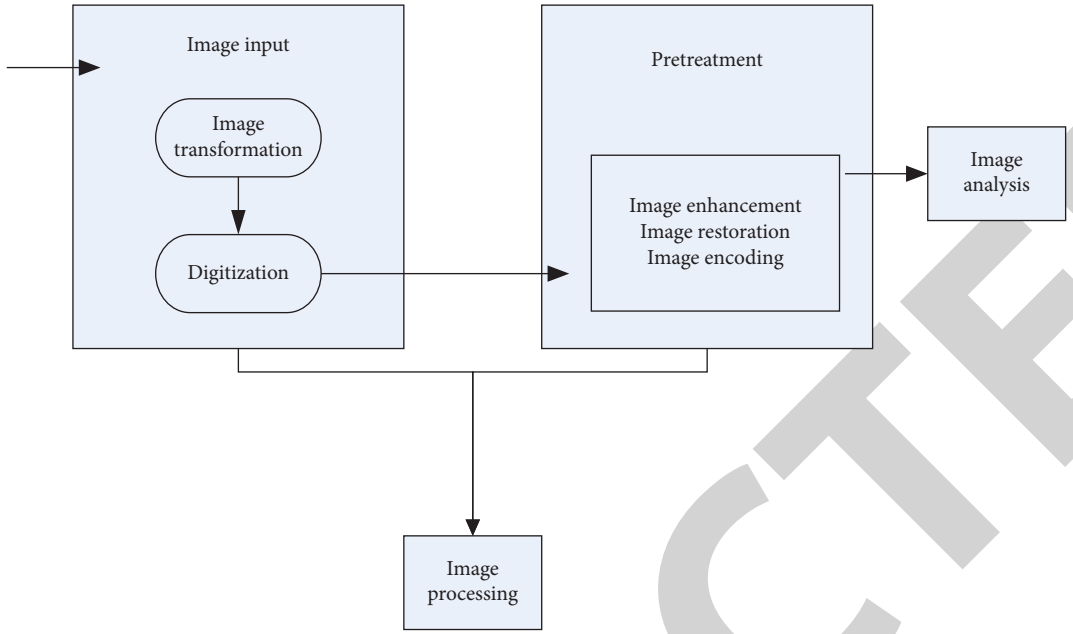

Figure 4: Main contents of digital image processing.

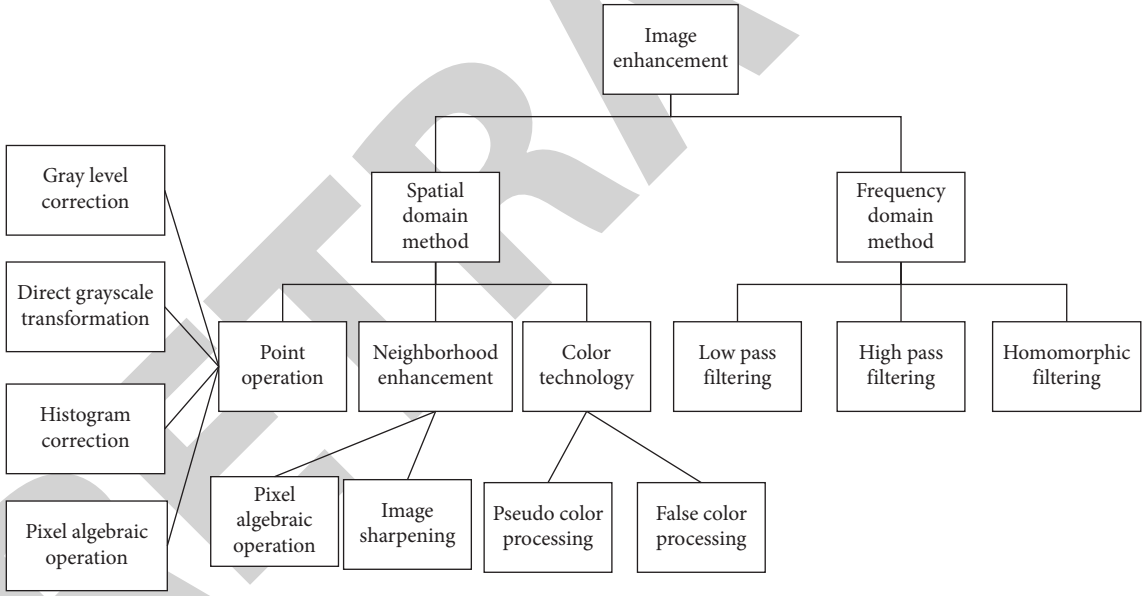

Figure 5: Main classification of digital image enhancement methods.

extracted features can include many aspects, such as frequency-domain features, grayscale or color features, boundary features, regional features, texture features, shape features, topological features, and relational structures.

It can be known from the convolution theorem that if the original image data information is $p(x, y)$, $q(x, y)$ is the processed image, and the unit impulse response in the system is $h(x, y)$, then

$$q(x, y) = p(x, y) * h(x, y). \tag{1}$$

In the above formula, $*$ represents convolution. After Fourier transform, $p(x, y)$, $q(x, y)$, and $h(x, y)$ are converted into $P(m, n)$, $Q(m, n)$, and $H(m, n)$, respectively. This is

$$Q(m, n) = P(m, n)H(m, n). \tag{2}$$

In the above formula, $H(m, n)$ is the transfer function.

In the enhancement problem, suppose the original image data information is $p(x, y)$ and $P(m, n)$ is the processed image data information obtained through Fourier transform, then select the appropriate $H(m, n)$, so that

$$q(x, y) = Q^{-1}[P(m,n)H(m,n)]. \quad (3)$$

In image processing, the conversion of grayscale contrast can be used to change the grayscale value obtained by the image data. For the input image, the output image will be generated after the gray-scale contrast conversion, and the gray value of each output image is only determined by the gray value of the corresponding input signal. The contrast enhancement method is suitable for images with low contrast. The image enhancement is achieved by modifying the gray scale of each pixel through linear and nonlinear changes, thus changing the dynamic range of the image.

Supposing the image is $p(x, y)$, the processed image is $q(x, y)$, and the conversion of gray-scale mapping is represented by S, then the contrast enhancement can be represented as

$$q(x, y) = S[p(x, y)]. \quad (4)$$

(1) Linear Transformation. Suppose the grayscale range of the raw image $p(x, y)$ is $[x_1, x_2]$, and now you want the grayscale range of the converted image to be $[x_3, x_4]$. Then, we have the conversion

$$q(x, y) = \frac{x_4 - x_3}{x_2 - x_1}[p(x, y) - x_1] + x_3. \quad (5)$$

The specific relationship image is shown in Figure 6(a).

(2) Piecewise Linear Transformation. In general, in order to emphasize the desired information of the image, it is necessary to expand the area, stretch some gray values, and reduce the unnecessary gray areas at the same time. This is called piecewise linear transformation. Figure 6(b) shows a schematic diagram of piecewise linear transformation.

The corresponding mathematical expression is

$$q(x, y) = \begin{cases} \frac{x_3}{x_1} p(x, y), & 0 \le p(x, y) \le x_1, \\ \frac{x_4 - x_3}{x_2 - x_1}[p(x, y) - x_1] + x_3, & x_1 \le p(x, y) \le x_2, \\ \frac{M_q - x_4}{M_p - x_2}[p(x, y) - x_2] + x_4, & x_2 \le p(x, y) \le M_p. \end{cases} \quad (6)$$

In Figure 6, the gray scale interval $[x_1, x_2]$ is linearly expanded, while the gray scale interval $[0, x_1]$ and $[x_2, M_p]$ are linearly compressed.

(3) Nonlinear Transformation. Nonlinear transformation uses the mathematical properties of the transfer function to achieve the compression and expansion of different grayscale intervals. The following is a brief introduction to logarithmic expansion and exponential expansion.

The mathematical expression for logarithmic expansion is

$$\begin{aligned} q(x, y) &= \lg[p(x, y)], \\ q(x, y) &= C\lg[p(x, y) + 1]. \end{aligned} \quad (7)$$

In the above formula, the natural logarithm is selected as the base, C is the scale ratio coefficient; and $p(x, y) + 1$ is to avoid finding the logarithm of zero. The function curve of logarithmic expansion is shown in Figure 7(a).

Logarithmic expansion can greatly compress the high grayscale area of the image, while reducing the low grayscale area of the image, making the details of the grayscale range easier to see. When the original image dynamic range is relatively large, it may exceed the display range of the display device, so logarithmic expansion of the original image is required to achieve the purpose of compressing grayscale.

The mathematical expression for exponential expansion is

$$q(x, y) = t^{p(x,y)}. \quad (8)$$

Adding modulation parameters to it, we get

$$q(x, y) = t^{x_3[p(x,y)-x_1]} - 1. \quad (9)$$

In the above formula, x_1 is the starting position of the curve, and x_3 is the rate of change of the curve. The three parameters x_1, x_2, and x_3 can adjust the position and shape of the curve. The effect of exponential expansion on the image is opposite to that of logarithmic expansion. The function curve is shown in Figure 7(b).

In digital image processing, the grayscale histogram reflects the distribution of image grayscale. Assuming that the gray distribution density function of the image at point $p(x, y)$ is $f(g; x, y)$, then the gray distribution density function of the image is

$$f(g) = \frac{1}{S}\iint_D f(g; x, y)\mathrm{d}x\,\mathrm{d}y. \quad (10)$$

In the above formula, D is the domain of the image and S is the area of the region D.

In general, it is very difficult to accurately obtain the gray-scale density distribution function $f(g)$ of the image, so the gray-scale histogram of the digital image is used to approximate it. Supposing the total number of pixels of a digital image is n, the total number of pixels of gray level r_i where the i-th gray level appears in the image is n_i, n_i/n is the frequency, and L is the total number of gray levels. Then, the probability of the i-th gray level is

$$f_r(r_i) = \frac{n_i}{n}\left(0 \le r_i \le 1, k = 0, 1, 2, \ldots, L(L-1)\right). \quad (11)$$

The abscissa of the grayscale histogram is the gray level, and the ordinate is the frequency of the gray level. But the histogram only reflects the overall grayscale distribution of the image, but it cannot show the spatial information and detailed features of the image. Histogram equalization has a good enhancement effect for images that have a large frequency in the low-value gray interval and where details are not clearly visible in the

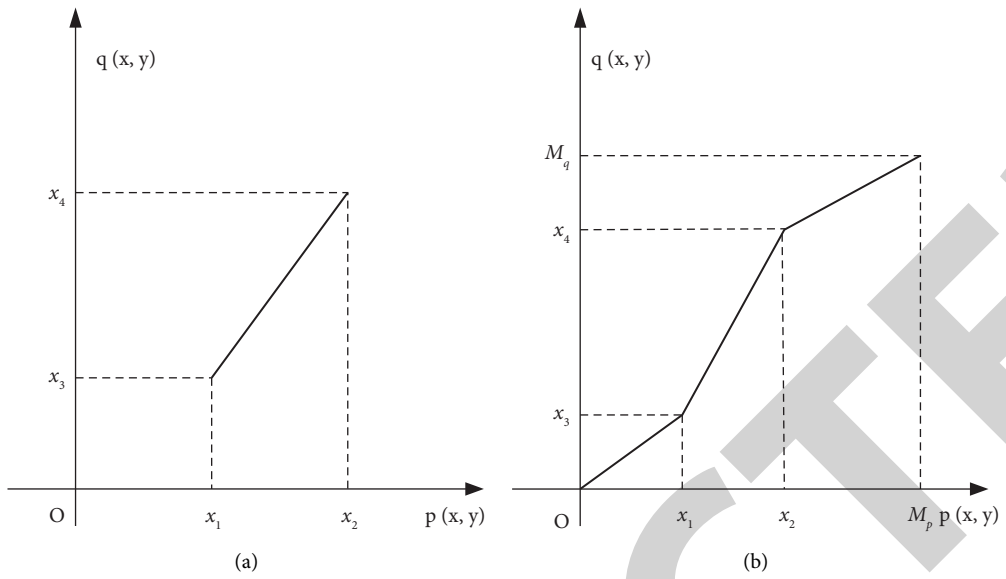

Figure 6: Specific relationship between linear transformation (a) and piecewise linear transformation (b).

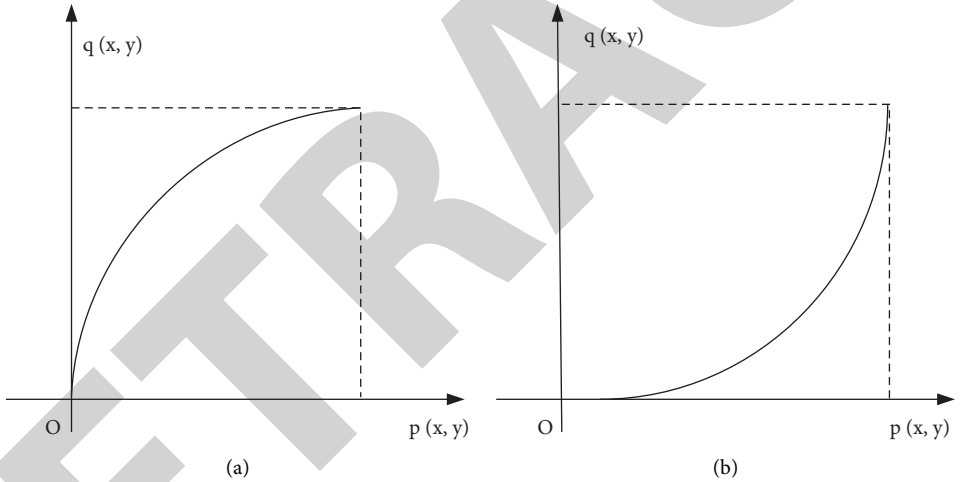

Figure 7: Function curve of logarithmic expansion (a) and exponential expansion (b).

darker areas of the image. In order to display an image effect with a relatively large dynamic range and rich gray levels, some transformation can be applied during the processing so that the histogram of the transformed image occupies the entire gray level range and is evenly distributed. This enhancement technique is called histogram equalization.

Let s and t be the gray level of the original image and the gray level of the image after histogram equalization. To facilitate discussion, normalize s and t to

$$0 \le s, t \le 1. \tag{12}$$

$t = T[s]$ is the transformation performed on the r value of the interval [0, 1], which should meet the following conditions:

(a) When $0 \le s \le 1$, $T[s]$ is a monotonically increasing function

(b) When $0 \le s \le 1$, $0 \le t = T(s) \le 1$.

The abovementioned condition (a) the monotonic increase requirement of $T[s]$ guarantees the existence of its inverse transformation; condition (b) ensures that the transformed pixel gray scale is within the allowable range.

Assuming that the probability density functions before and after the transformation are $p_s(s)$ and $p_t(t)$ respectively. The purpose is to transform $T[s]$ to make the histogram

evenly distributed, that is, $p_t(t)$ is a constant, and $p_t(t) = 1$ can be set.

Since the physical definition of the histogram is the number of pixels with grayscale size, the part of the histogram represents the total number of grayscale pixels, and its value should be equal to the total number of pixels in the corresponding grayscale after conversion, so

$$\int_0^t p_t(t)dt = \int_0^s p_s(s)\mathrm{d}s. \tag{13}$$

Assuming that there is already $p_t(t) = 1$, then there is

$$t = \int_0^t 1\,dt = \int_0^s p_s(s)\mathrm{d}s. \tag{14}$$

It can be seen from above that by making the transformed gray scale t equal to the cumulative distribution function of the gray scale s before the transformation, that is,

$$T(r) = \int_0^s p_s(s)\mathrm{d}s. \tag{15}$$

$p_t(t)$ can be realized, that is, the transformed histogram is uniformly distributed.

We replace the probability value with the frequency of the gray level s_i, that is,

$$p_i(s_i) = \frac{n_i}{n}\,(0 \le s \le 1; \quad i = 0, 1, ..., L(L-1)). \tag{16}$$

In the above-given formula, n is the total number of pixels in the image, n_i is the number of times the i-th gray level appears, $p_i(s_i)$ is the probability of taking the i-th gray level, and L is the total number of gray levels.

The cumulative distribution function of formula (16), which is the so-called discrete gray scale transformation function, is

$$T_i = T(s_i) = \sum_{j=0}^{i} \frac{n_j}{n}\left(0 \le s_i \le 1; k = 0, 1, ..., L(L-1)\right). \tag{17}$$

The above formula maps each pixel whose gray level is s_i in the original image to the corresponding pixel whose gray level is t_i in the new image.

The image enhancement effect after histogram equalization is not easy to control. Finding a gray scale conversion function according to the histogram of the known image, which can control the change of the gray value. This technique is called histogram specification. Therefore, in order to achieve a better image effect, only an appropriate functional relationship needs to be selected.

Supposing the histogram of the original image is $p_s(s)$, and the prescribed histogram is $p_g(g)$. Equalize the image with histogram, and set

$$\begin{cases} s = T[s] = \int_0^s p_r(x)\mathrm{d}x, \\ t = G[g] = \int_0^g p_g(x)\mathrm{d}x. \end{cases} \tag{18}$$

Then, there is

$$p_s(s) = p_t(t) = 1, 0 \le s, t \le 1. \tag{19}$$

Statistically speaking, s and t are exactly the same, so it can use s instead of t and then take the inverse transformation to get

$$g = G^{-1}(t). \tag{20}$$

The steps of digital image histogram specification are as follows:

$$\begin{aligned} p_i &= \sum_{k=0}^{i} p_g(k), i = 0, 1, ..., L(L-1), \\ p_j &= \sum_{l=0}^{j} p_g(l), j = 0, 1, ..., L(L-1). \end{aligned} \tag{21}$$

Then, perform the transformation of $i \longrightarrow j$ according to the principle of closest to $p_i \longrightarrow p_j$, find the transformation function of $i \longrightarrow j$, and perform gray-scale transformation on the original image.

$$j = T(i). \tag{22}$$

In the above formula, $p_s(i)$ is the histogram of the original digital image, $p_g(j)$ is the prescribed histogram, and the value range of i and j is $i, j = 0, 1, ..., L(L-1)$.

This paper uses DKI imaging parameters to analyze the clinical symptoms of cervical spondylotic myelopathy, which helps to improve its accuracy and optimize its image efficiency. Image analysis is also called image recognition, which is important for analyzing the elements of interest in the image, processing their position information, and setting the image description at the same time. The main process of image recognition is shown in Figure 8:

2.3. Treatment of Spinal Cord Type Cervical Spondylosis. Patients with mild cervical spondylotic myelopathy generally choose conservative treatments such as a combination of Chinese and Western medicine and exercise, which have a better effect on reducing symptoms and delaying the progression of the disease. However, for patients with relatively severe disease and impaired spinal function, surgical treatment should be considered. The following is a detailed introduction to the two treatment methods:

2.3.1. Conservative Treatment. The purpose of conservative treatment is to alleviate the patient's symptoms, protect the function of the spinal cord, and slow down the progression of the disease. It generally includes medication, physical therapy, and other methods. Nonsteroidal antiinflammatory drugs are commonly used to relieve neck and shoulder pain

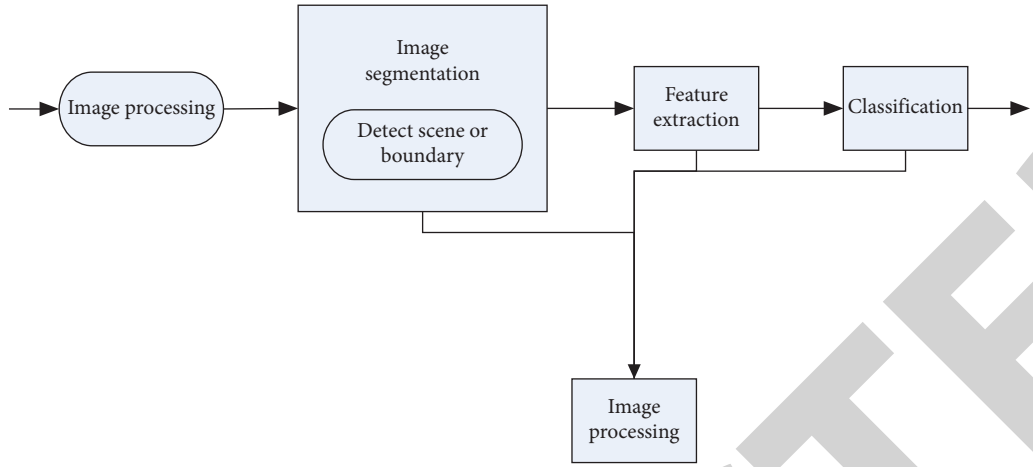

Figure 8: Main process of image recognition.

and limb pain. Such drugs can reduce inflammation, reduce nerve edema, and have a significant relieving effect on acute symptoms. There are also traditional Chinese medicine and traditional Chinese medicine treatments for cervical spondylotic myelopathy. Therapies such as acupuncture, electroacupuncture, cupping, and traditional Chinese medicine can also achieve good therapeutic effects. In order to maintain the stability of the cervical spine, reduce the wearable neck circumference that may cause symptoms due to improper cervical spine activity. However, long-term wearing can cause atrophy of the back of the neck muscles. The back of the neck muscles should be properly exercised to maintain the function of the muscles themselves. Cervical spondylotic myelopathy is a relatively serious type of cervical spondylosis, because the anterior disc herniation or the calcification of the posterior longitudinal ligament, the hyperplasia of the side facet joints, or the hypertrophy of the ligamentum flavum, etc. cause compression of the cervical spinal cord, causing cervical spondylosis, which can cause cervical spondylosis. Diagnosis: History of cervical spine. The clinical manifestations of cervical spondylotic myelopathy are typically the feeling of stepping on cotton under the soles of the feet, the feeling of binding on the body, increased walking muscle tension, increased upper and lower extremity muscle tension, and decreased hand flexibility.

2.3.2. Surgical Treatment. Due to the natural course of cervical spondylotic myelopathy, many patients will continue to deteriorate during treatment. As long as the operation is suitable, it is best to perform the operation within 6 months, because usually after 6 months or more, the effect after the operation is not good. The purpose of surgery is to eliminate the compression of the spine, restore or reshape the height of the spinal cord and intervertebral discs, while maintaining the stability of the spine as much as possible, creating ideal conditions for the recovery of spinal function. The most common surgical procedures in the clinic mainly include the following.

Anterior surgery: the key points of the surgical process and technique of cervical discectomy and fusion fixation (ACDF) are that in China, the front and right sides of the neck are generally used to cut the skin and cut open the platysma. The gap between the cervical vascular sheath and the visceral sheath at the medial edge of the sternocleidomastoid muscle is separated to the front of the vertebral body. C-arm fluoroscopy confirms the operation segment and expands the intervertebral disc, removes the intervertebral disc, and cleans the osteophytes on the posterior edge of the vertebral body. The upper and lower endplates of the vertebrae were scraped to spot hemorrhage. An iliac bone block or intervertebral fusion cage was inserted between the vertebrae, and the vertebral body was fixed with titanium plate screws. Anterior surgery can directly remove the compressed intervertebral discs in the front of the spine, such as damaged intervertebral discs and herniated intervertebral discs, osteophytes on the spine, and short ossified longitudinal ligaments, and can widen narrowed intervertebral discs to maintain the stability of the spine. However, the risk of anterior surgery is higher, and there is a risk of injury to the esophagus, trachea, vertebral artery, and laryngeal nerve during the operation. Multisegment segmentation and fixation may reduce the recovery of the cervical spine and increase the risk of degeneration of nearby segments.

Posterior surgery: when the cervical spine has a physiological lordosis, the spinal cord will float to the rear with less tension after decompression via the posterior approach, which is the "bowstring principle." This method is an indirect decompression for the compressive substance on the ventral side of the spinal cord, and it can also relieve the hypertrophy of the ligamentum flavum on the dorsal side of the spinal cord. However, this surgical method should be used with caution when the curvature of the cervical spine becomes straight or recurved. The more commonly used surgical methods for posterior cervical surgery are laminectomy and laminoplasty. Laminectomy decompresses the spinal cord sufficiently and thoroughly but completely

removes the lamina and destroys the posterior structure of the cervical spine. Postoperative cervical kyphosis may occur, and surrounding scar formation can compress the spinal cord again. Therefore, total posterior cervical laminectomy and decompression surgery are currently less clinically used. With the development of internal fixation materials and technology, the current clinical application is the posterior cervical laminectomy decompression via lateral mass screw rod system internal fixation. The prevention of cervical kyphosis after side mass fixation is beneficial to the recovery of spinal cord function. An evidence-based medical study found that the efficacy of laminectomy and fusion in the treatment of cervical spondylotic myelopathy and ossification of the posterior longitudinal ligament of the cervical spine is similar to that of laminectomy and laminoplasty. However, compared with laminectomy, no cervical kyphosis occurs, so this procedure is safer and more effective. Although laminectomy, decompression, and internal fixation can achieve good clinical results, the operation time is prolonged during the operation, the long-segment fixation reduces the mobility of the cervical spine, and there is a risk of internal fixation failure. Laminoplasty is a commonly used procedure for the treatment of multisegment cervical spondylotic myelopathy.

Posterior cervical surgery is relatively simple and has low intraoperative risks. It is especially suitable for patients with multisegment cervical spondylotic myelopathy, but it is generally not suitable for patients with cervical spine instability.

Anterior and posterior combined surgery: cervical anterior and posterior combined decompression and fixation is generally suitable for patients with both abdominal and dorsal spinal cord compression, multisegment cervical spondylotic myelopathy combined with cervical spine instability, or cervical spine reflex. However, this surgical method is relatively traumatic, and the operation time is longer. It should be carefully selected for patients with poor general conditions.

Minimally invasive surgery: with the promotion of minimally invasive concepts and the development of spine minimally invasive techniques, minimally invasive techniques have been gradually applied in the treatment of cervical spondylosis. Commonly used cervical minimally invasive techniques include radiofrequency thermal coagulation targets, percutaneous laser disc decompression, and microendoscopic discectomy. Minimally invasive surgery has the advantages of less trauma and quick recovery, but it also uses stricter surgical indications. It is believed that with the advancement of technology, minimally invasive surgery will get more development.

2.3.3. Choice of Surgical Method. The choice of surgical method needs to consider the patient's clinical manifestations, imaging characteristics, age, whether there are comorbidities, whether there are bad habits (such as smoking), and the experience and preferences of the surgeon. However, some clinical features have been widely recognized for guiding the choice of surgery. Generally, the spinal cord compressive material is located on the ventral side (such as herniated discs and osteophytes on the posterior edge of the vertebral body), the compression does not exceed 3 segments, the cervical spine is unstable, and the cervical spine curvature is often selected for anterior surgery. The posterior approach is often chosen when the spinal cord pressure is located on the dorsal side (such as in the hyperplastic and hypertrophic ligamentum flavum) and compresses 3 or more segments. Some patients' bad behaviors, such as smoking, may affect the outcome of surgery. In particular, it can lead to nonunion of bones and movement of false joints after anterior cervical bone grafting. Postoperative axial symptoms are a common complication after posterior cervical spinal canalplasty. Patients with cervical spondylotic myelopathy who have clinically significant neck pain before surgery should be cautious when choosing this procedure.

The main purpose of cervical spondylotic myelopathy surgery is to improve the pressure on the spinal cord and nerve roots while minimizing damage to the spinal system and reducing the occurrence of complications after surgery. It is generally believed that anterior surgery is suitable for single-segment spinal cord lesions. In this way, the foreign body can be removed directly at the location of the lesion, and the trauma to the patient's affected area is less. However, it is not suitable for the treatment of multisegment lesions, which increases the risk of complications such as damage to adjacent segments, joint failure, and false joints. In many classic surgical operations on the posterior cervical spine, the long-term effect is relatively stable, but the damage to the spine structure is the greatest. Therefore, the use of endoscopic cervical posterior surgery can reduce the damage to the spinal cord, reduce the occurrence of complications, and achieve the purpose of reduction.

3. Feature Recognition of Clinical Symptoms of Cervical Spondylotic Myelopathy

In this paper, we investigated and analyzed the conditions of 30 patients with cervical spondylosis in a central hospital, of whom 30–60 years were classified as mild (37 cases) and moderate (23 cases) according to the Japanese Orthopaedic Association's 17-point spinal cord damage functional assessment scale (JOA score). 0–4 points were considered severe damage, 5–8 points were considered severe damage, 9–12 points were considered moderate damage, 13–16 points were considered mild damage, and 17 points were considered normal function. The score was a normal function. Routine sagittal T1WI, T2WI, and STIR sequences, axial T2WI sequences, and DKI sequences were performed. The mean diffusion coefficient (MD) and mean diffusion kurtosis (MK) were measured separately.

In order to study the clinical symptoms of cervical spondylotic myelopathy, from which six patients with cervical spondylosis were selected for investigation and analysis, and we randomly selected 6 healthy volunteers for comparative experiments. The patients and healthy volunteers are between 30 and 50 years, and the average

age is the same at 45 years. All subjects had normal cervical MRI scans. And we let them all perform movement checks in the three directions of the cervical spine in the neutral position, the hyperextension position, and the hyperflexion position. We used the T2WI axis to detect the transverse axis of the cervical intervertebral disc in each state. We used the PACS system measurement tool to measure the dynamic data of C1/2, C2/3, C3/4, C4/5, C5/6, C6/7, and C7/8 horizontal disc bulge sizes. Each subject in this study understands the content of the study and signed an information confirmation form at the same time.

Among them, the requirements for entering the healthy volunteer group are as follows: (1) There is no obvious displacement artifact in the detection image. (2) No clinical symptoms and signs of cervical spondylosis and spondylopathy. (3) Routine MRI examination of the cervical spine showed no abnormalities. (4) There were no bad habits, no obvious obesity, etc., and they showed good cooperation. (5) No serious cervical spine injury event and related trauma history.

Before the scan, the patient's head was placed in a cranial fixation frame and fixed and braked during the MRI examination. It prevents movement artifacts due to movement. Wear special sponge earplugs for the patient to reduce the impact of noise on the patient. In the normal neutral position, the head is advanced in the natural supine position. In the hyperextension position, use cotton pads to raise the shoulders as much as possible to allow the neck to recline to the maximum. Put cotton pads on the occiput in the overflexion position to allow the mandible to be retracted to the maximum, as close as possible to the stem of the sternum. Before the scan, instruct the patient to keep breathing as calmly as possible during the examination and avoid coughing and swallowing.

In the study, superconducting MRI was performed on each subject, and the DKI imaging parameters of the DKI spinal cord and the model Philips INGEnia-CX 3.0 T superconducting MRI were as follows: repetition time/echo time, 3000/91 ms; number of excitations, 2; layer thickness/layer spacing, 4/0 mm; number of layers: 17; FOV, 230×230 mm; spatial separation resolution, $1.3 \times 1.3 \times 4.0$; three b-values (0, 1000, and 2000 s/mm^2), each coded in 20 diffusion directions. All cases underwent a routine neutral MRI examination. It includes sagittal TSE-T2WI scan (TR/TE = 3500 ms/96 ms, NEX = 2, slice thickness 3.0 mm, slice distance 0.3 mm, FOV23 cm) and TSE-T2WI scan (TR/TE = 2000 ms/78 ms, NEX = 2, layer thickness 3.0 mm, layer spacing 0.3 mm, FOV 16 cm). The cross-sectional scan images all included C1/2, C2/3, C3/4, C4/5, C5/6, C6/7, and C7/8 intervertebral disc central plane. The sequence selected for the hyperextension and overflexion MRI examinations is the same, namely, sagittal TSE-T2WI scan (TR/TE = 3500 ms/96 ms, NEX = 2, slice thickness 3.0 mm, slice distance 0.3 mm, FOV 23 cm) and cross-sectional TSE-T2WI scan (TR/TE = 2000 ms/78 ms, NEX = 2, layer thickness 3.0 mm, layer spacing 0.3 mm, FOV 16 cm). In the transverse position, scan one layer of the central layer of the intervertebral disc from C1/2 to C7/8. In dynamic MRI scans of each posture, a presaturation zone was added to the front of the cervical vertebral body.

The processing of cervical spine MRI images in each posture after obtaining the data images of the examinee. Take the midsagittal T2WI as the positioning image. Mark the C1/2, C2/3, C3/4, C4/5, C5/6, C6/7, and C7/8 intervertebral disc cross-sectional T2WI images. Use the PACS system measurement tool to measure the dynamic data of C1/2, C2/3, C3/4, C4/5, C5/6, C6/7, and C7/8 horizontal disc bulge size. All data are measured on the median sagittal and axial T2WI images.

The collected digital image contains a lot of random noise. If it is directly denoised and a single frame of digital image is enhanced, it will lose a lot of useful information while removing the noise. Therefore, if it is possible to obtain continuous multiframe radiographic images, the multiframe superposition method is generally used to remove random noise first, and then the correlation enhancement processing is performed. In order to verify the effectiveness of the digital image enhancement technology proposed in the thesis, this paper processes the cervical spine MRI images after the data images of patients with cervical spondylotic myelopathy.

4. Clinical Symptoms of Cervical Spondylotic Myelopathy

4.1. Comparison of MD Values and MK Values between the Healthy Volunteer Group and the Patient Group. The comparison of MK values and MD values in the spinal cord between the normal group and the patient group is shown in Table 1 and Figure 9. The comparison of MD values and MK values in different groups showed that the MD values and MK values in the patient group were lower than those in the normal group, and the differences were all statistically significant ($p < 0.05$).

In this study, all patients had different degrees of clinical symptoms, and no significant abnormal signals were seen in the spinal cord. Increased MK values indicated that the microstructure became more complex, the degree of diffusion restriction was more obvious, and the deviation from Gaussian distribution displacement was greater. The MD and MK values in this study were positively correlated with the JOA score, reflecting the trend of gradual decrease of MK values and gradual increase of MD values as the clinical symptoms of spinal cord-type cervical spondylosis worsened. It may reflect further injury damage to neurons and a further increase in local isotropy.

4.2. Image of Bulging Disc. We randomly extract a scanned image of the patient and perform an image enhancement experiment on the image in Figure 10(a) on the basis of image transformation. Figure 10(b) is the image after image enhancement processing using parameter ratio method and gray-level correction method.

It can be seen that the image of the patient after the instrument examination is relatively blurry. After image processing, the image becomes clear. It is conducive to our

Table 1: Means and comparison of MK and MD values in the healthy volunteer and patient groups.

Related indicators	MK value	MD value
Health volunteer group	1.02 ± 0.10	1.10 ± 0.069
Patient group	0.86 ± 0.07	0.98 ± 0.085

further research on the clinical symptoms of cervical disc C1/2, C2/3, C3/4, C4/5, C5/6, C6/7, and C7/8 segments

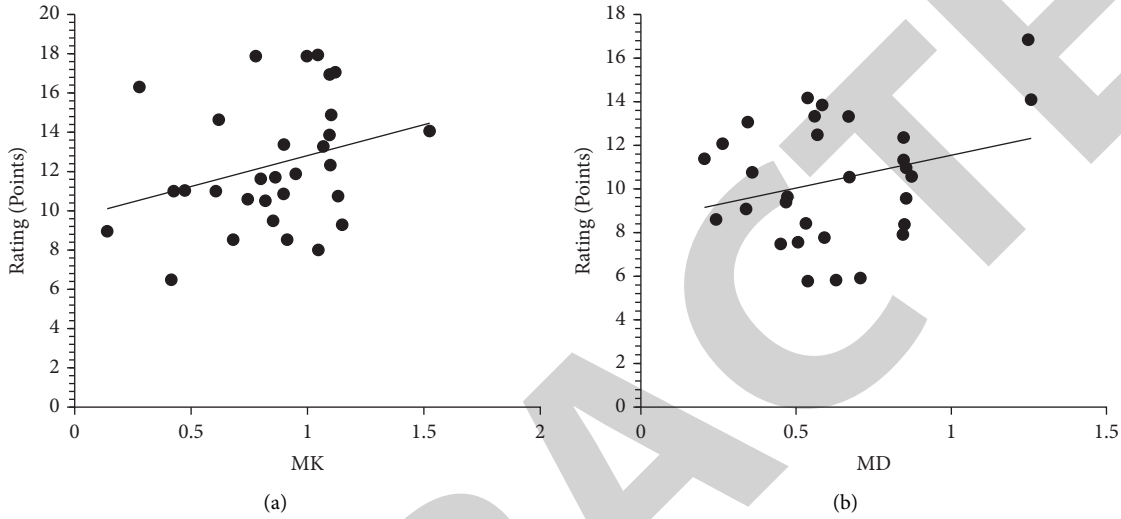

Figure 9: Scatter plot of correlation between MK and MD values and JOA scores. (a) $r = 0.528$, $p < 0.01$. (b) $r = 0.194$, $p < 0.01$.

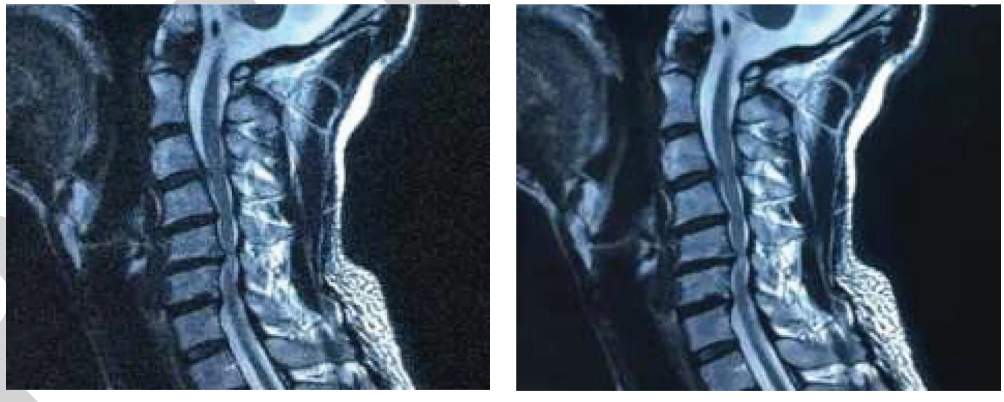

Figure 10: Comparison of image enhancement processing of intervertebral disc herniation. (a) Original cervical scanning image. (b) The image processed by image enhancement technology.

spondylotic myelopathy.

4.3. Comparison of the Size of Intervertebral Disc Bulging. Figure 11 shows the size of intervertebral disc bulging in the three states. It came from 12 subjects in the intervertebral in the hyperflexion, hyperextension, and neutral positions.

It can be seen from Figure 11 that the cervical spine of the cervical spondylotic myelopathy group and the healthy group are in an overflexed state. As the segment value increases, the cervical intervertebral disc bulge increases. In addition to the inconspicuous C1/2 segment, the cervical

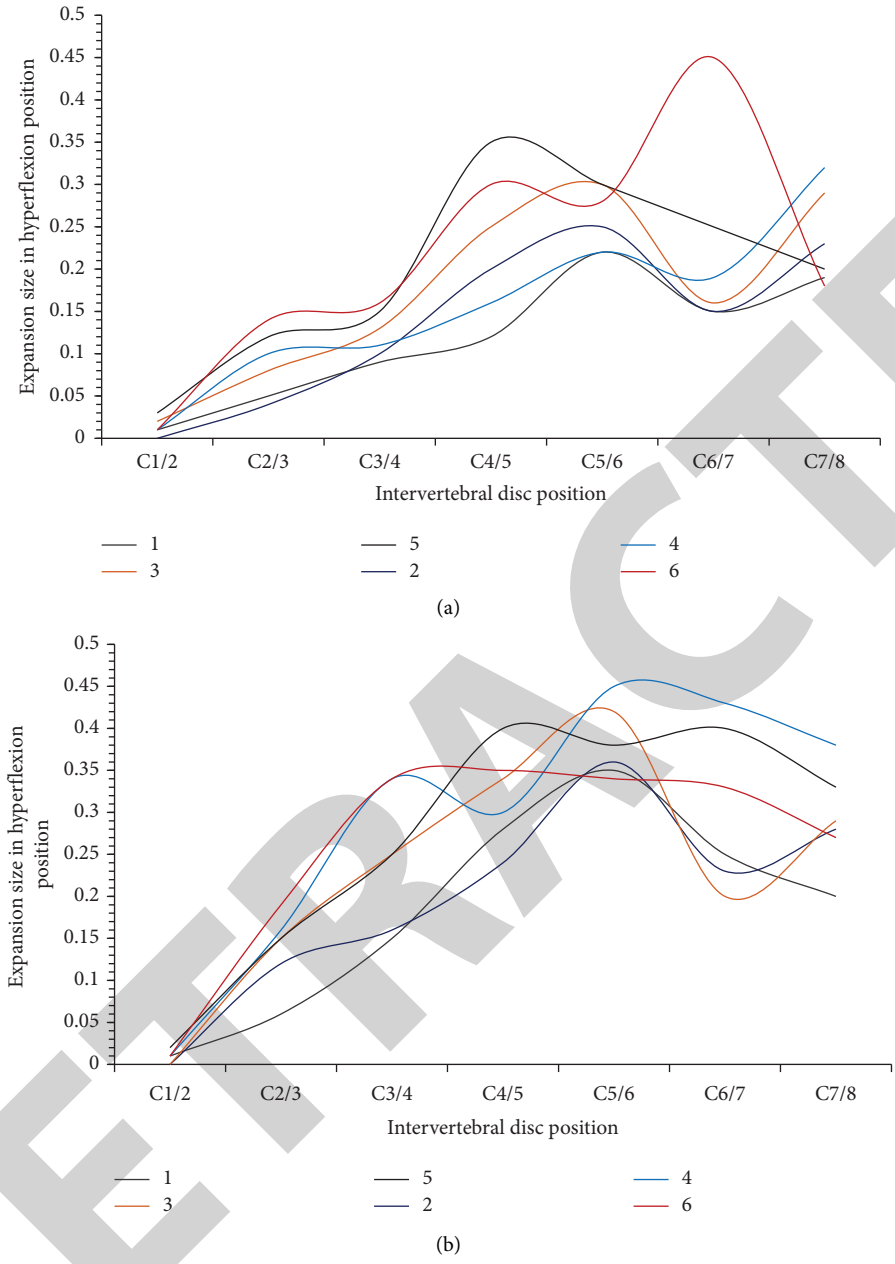

Figure 11: Comparison of the size of cervical disc herniation in different segments of cervical hyperflexion between the two groups. (a) Healthy group. (b) Patient group.

intervertebral disc bulge of each segment of the cervical spondylotic myelopathy group was larger than that of the healthy group.

It can be seen from Figure 12 that the cervical vertebrae of the cervical spondylotic myelopathy group and the healthy group are in a neutral position, and the cervical disc bulge in each of the other segments of the cervical spondylotic myelopathy group is larger than that of the healthy group. Except for the C1/2 and C2/3 segments, it is not obvious. The sixth patient's cervical disc bulge at C7/8 segment reached the highest value of 0.68.

From Tables 2 and 3, it can be seen that the cervical spine of the cervical spondylotic myelopathy group and the healthy group are in the hyperextension state, and the cervical disc bulge of each segment of the cervical spondylotic myelopathy group is larger than that of the healthy group. Regardless of the healthy group or the patient group, the size of cervical disc bulging is hyperextension position > neutral position > overflexion position.

4.4. Comparison of the Number of Bulging Discs. Tables 4 and 5 show the average detection rate of cervical intervertebral disc bulge in different segments in different positions in 12 cases of the control group. In different positions, the

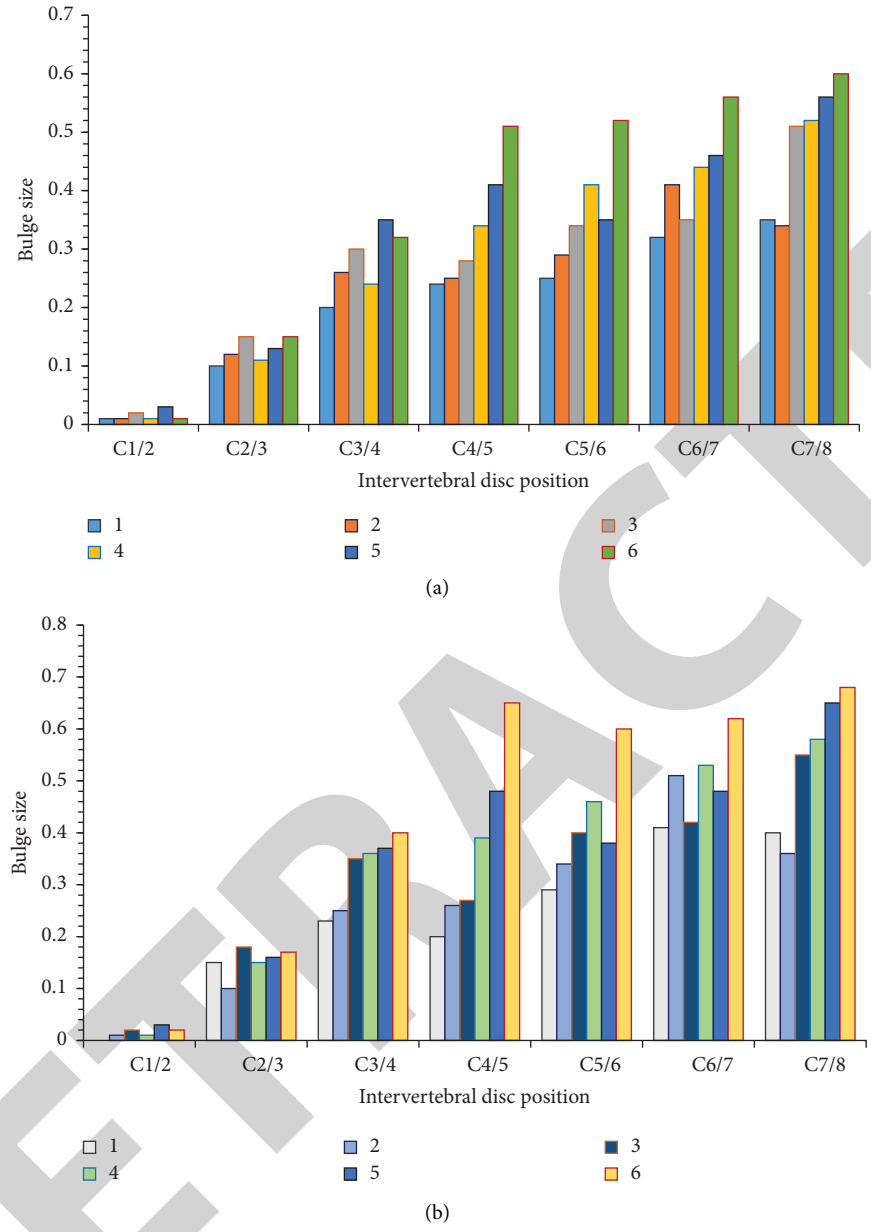

Figure 12: Comparison of the size of cervical disc herniation at different segments in the neutral position between the two groups. (a) Healthy group. (b) Patient group.

Table 2: Size of cervical disc herniation at different segments of cervical hyperextension in 6 healthy subjects.

Intervertebral disc segment	1	2	3	4	5	6
C1/2	0	0.02	0.02	0.01	0.03	0.02
C2/3	0.33	0.35	0.39	0.24	0.30	0.29
C3/4	0.46	0.52	0.55	0.42	0.46	0.49
C4/5	0.56	0.26	0.34	0.39	0.50	0.48
C5/6	0.37	0.36	0.48	0.49	0.48	0.61
C6/7	0.43	0.58	0.45	0.55	0.50	0.79
C7/8	0.50	0.53	0.56	0.60	0.68	0.78

percentage of cervical disc bulging in the patient group was about 2% higher than that in the healthy group. Among them, the detection rate of disc bulging in the hyperextension position is the highest, reaching 27%.

Table 3: Size of cervical disc herniation at different segments of cervical hyperextension in 6 subjects in the patient group.

Intervertebral disc segment	1	2	3	4	5	6
C1/2	0	0.03	0.03	0.03	0.03	0.02
C2/3	0.38	0.40	0.42	0.32	0.38	0.32
C3/4	0.51	0.48	0.56	0.48	0.52	0.54
C4/5	0.60	0.31	0.35	0.47	0.55	0.50
C5/6	0.41	0.46	0.44	0.58	0.64	0.76
C6/7	0.52	0.74	0.65	0.60	0.55	0.81
C7/8	0.52	0.64	0.60	0.75	0.74	0.82

Table 4: Comparison of the number and percentage of cervical disc herniation in 6 cases of healthy group in different positions.

Cervical posture	1 (%)	2 (%)	3 (%)	4 (%)	5 (%)	6 (%)	Average value (%)
Over flexion position	5	6	5	7	8	5	6
Neutral bit	13	10	15	16	13	14	13.5
Hyperextension position	28	25	24	26	24	25	25.3

Table 5: Comparison of the number and percentage of cervical disc herniation in 6 patients with different positions of cervical spine in the patient group.

Cervical posture	1 (%)	2 (%)	3 (%)	4 (%)	5 (%)	6 (%)	Average value (%)
Over flexion position	7	9	10	8	9	6	8.17
Neutral bit	14	15	15	16	15	17	15.33
Hyperextension position	29	27	25	28	26	27	27

In the human spine, the cervical spine is the part with the largest range of motion. When the cervical spine is moving, the shape and size of soft tissues such as bony spinal canal, intervertebral disc, dural ligament, spine and ligament will cause corresponding changes. Traditional MRI of the cervical spine in the supine position cannot fully and accurately assess the actual situation of the spine and its internal spinal cord. It shows the relative relationship between the spinal cord and its contents. Dynamic MRI examination of the cervical spine has obvious advantages. In the examination of the disc bulge in this study, the T2WI signal of the cervical disc was weakened. This is consistent with the fact that bulging of the intervertebral disc is caused by fluid loss and decreased elasticity during spinal cord injury. Cervical hyperextension imaging showed a significant increase in the size and number of cervical disc herniation (especially the discs with greater disc activity in C4/5, C5/6, and C6/7 segments), which increased by 0.82 and 27%, respectively. The posterior longitudinal ligament is relaxed in the hyperextension position of the cervical spine and cannot accommodate the intervertebral disc tissue space.

5. Conclusion

Spinal cord cervical spondylosis is a very common type of cervical spondylosis and is the most dangerous of all. Once cervical spondylotic myelopathy develops to the middle and late stages, surgical treatment will cause irreversible damage to spinal function. Therefore, how to diagnose and accurately diagnose spinal cord injury early and determine clinical symptom recognition is of great significance to treatment and prognosis. This paper introduces the parameter ratio method of diffusional kurtosis imaging and focuses on the analysis of cervical spine MRI image enhancement processing after obtaining the data images of the subject. In this paper, we found that in spinal cord type cervical spondylosis, DKI can reflect the microscopic pathophysiological changes of spinal cord injury, and the degree of change of MK value can reflect the degree of spinal cord injury, and we obtained data on the dynamic changes of the degree of C1/2, C2/3, C3/4, C4/5, C5/6, C6/7, and C7/8 of the cervical spine in normal subjects. It provides valuable imaging information for the study of dynamic physiology of normal cervical spine. Due to time and personal abilities, there are many areas for improvement in research. The main shortcomings are as follows: (1) The sample size is small, and the age range of the 12 healthy volunteers in this study is not large enough, and there are certain errors in the statistical analysis. (2) The data measured in this test are all experimental data manually measured in the comparative experiment, and there is a certain measurement error. (3) In this study, only part of the tissue structure of the cervical spine intervertebral disc was selected as the research object. It cannot fully demonstrate the pathophysiological changes of the spinal cord and the specific clinical symptoms of the patient.

Data Availability

Data sharing not applicable to this article as no datasets were generated or analyzed during the current study.

Conflicts of Interest

The authors declare no conflicts of interest.

References

[1] K. Ninomiya, T. Shiraishi, R. Aoyama et al., "Analysis of the impact of spinopelvic radiographic parameters on the severity of cervical spondylotic myelopathy," *Journal of Orthopaedic Science*, vol. 25, no. 6, pp. 966–974, 2020.

[2] H. Chang, C. Kim, and B. W. Choi, "Selective laminectomy for cervical spondylotic myelopathy: a comparative analysis with laminoplasty technique," *Archives of Orthopaedic and Trauma Surgery*, vol. 137, no. 5, pp. 611–616, 2017.

[3] D. H. Massel, V. Puvanesarajah, B. C. Mayo et al., "Surgical decision making in cervical spondylotic myelopathy: comparison of anterior and posterior approach," *Contemporary Spine Surgery*, vol. 17, no. 8, pp. 1–5, 2016.

[4] E. Yu, N. Romero, T. Miles, S. Hsu, and D. Kondrashov, "Dyspnea as the presenting symptom of cervical spondylotic myelopathy," *Surgery Journal*, vol. 02, no. 04, pp. e147–e150, 2016.

[5] R. K. J. Murphy, P. Sun, J. Xu et al., "Magnetic resonance imaging biomarker of axon loss reflects cervical spondylotic myelopathy severity," *Spine*, vol. 41, no. 9, pp. 751–756, 2016.

[6] H. Y. Chen, M. H. Yang, Y. P. Lin, F. H. Lin, P. Q. Chen, and S. H. HuYang, "Impact of cervical sagittal parameters and spinal cord morphology in cervical spondylotic myelopathy status post spinous process-splitting laminoplasty," *European Spine Journal*, vol. 29, no. 5, pp. 1052–1060, 2020.

[7] Y. Yang, T. Chen, W. Wu, and H. Zheng, "Modelling the stability of a soil-rock-mixture slope based on the digital image technology and strength reduction numerical manifold method," *Engineering Analysis with Boundary Elements*, vol. 126, pp. 45–54, 2021.

[8] T. G. Lee, K. H. Kim, T. Y. Kim et al., "Clinical study on 2 cases of cervical spondylotic myelopathy treated by Korean traditional medicine," *Journal of Korean Medicine Rehabilitation*, vol. 29, no. 3, pp. 141–148, 2019.

[9] S. Alli, I. Anderson, and S. Khan, "Cervical spondylotic myelopathy," *British Journal of Hospital Medicine*, vol. 78, no. 3, pp. C34–C37, 2017.

[10] Y. Imajo, T. Taguchi, M. Neo et al., "Surgical and general complications in 2,961 Japanese patients with cervical spondylotic myelopathy: comparison of different age groups," *Spine Surgery and Related Research*, vol. 1, no. 1, pp. 7–13, 2017.

[11] M. Abdolmaleky, M. Naseri, J. Batle, A. Farouk, and L. H. Gong, "Red-Green-Blue multi-channel quantum representation of digital images," *Optik*, vol. 128, pp. 121–132, 2017.

[12] P. Shan and X. Lai, "Mesoscopic structure PFC~2D model of soil rock mixture based on digital image," *Journal of Visual Communication and Image Representation*, vol. 58, pp. 407–415, 2019.

[13] C. R. Jutzeler, A. Ulrich, B. Huber, J. Rosner, J. L. K. Kramer, and A. Curt, "Improved diagnosis of cervical spondylotic myelopathy with contact heat evoked potentials," *Journal of Neurotrauma*, vol. 34, no. 12, pp. 2045–2053, 2017.

[14] C. M. Jalai, N. Worley, G. W. Poorman, D. L. Cruz, S. Vira, and P. G. Passias, "Surgical site infections following operative management of cervical spondylotic myelopathy: prevalence, predictors of occurrence, and influence on peri-operative outcomes," *European Spine Journal*, vol. 25, no. 6, pp. 1891–1896, 2016.

[15] J. T. Zhang, J. Q. Li, R. J. Niu, Z. Liu, T. Tong, and Y. Shen, "Predictors of cervical lordosis loss after laminoplasty in patients with cervical spondylotic myelopathy," *European Spine Journal*, vol. 26, no. 4, pp. 1205–1210, 2017.

[16] L. Ma, "Research on distance education image correction based on digital image processing technology," *EURASIP Journal on Image and Video Processing*, vol. 2019, no. 1, pp. 18-19, 2019.

[17] C. D. Witiw, L. A. Tetreault, F. Smieliauskas, B. Kopjar, E. M. Massicotte, and M. G. Fehlings, "Surgery for degenerative cervical myelopathy: a patient-centered quality of life and health economic evaluation," *The Spine Journal*, vol. 17, no. 1, pp. 15–25, 2017.

[18] H. Elnoamany, "Sensitivity of pyramidal signs in patients with cervical spondylotic myelopathy," *Asian Spine Journal*, vol. 10, no. 1, pp. 65–69, 2016.

[19] Z. Ma, X. Ma, H. Yang, H. Feng, and C. Chen, "Complex cervical spondylotic myelopathy: a report of two cases and literature review," *European Spine Journal*, vol. 25, no. S1, pp. 27–32, 2016.